

Effect of Pulse Widths and Cycles on Invasive, Bipolar, and Gated Radiofrequency-Induced Thermal Reactions in ex vivo Bovine Liver Tissue

Min Choi ¹, Hye Sun Lee ², Sung Bin Cho ³

¹R&D Center, Shenb Co., Ltd, Seoul, Korea; ²Department of Biostatistics, Yonsei University College of Medicine, Seoul, Korea; ³Yonsei Seran Dermatology and Laser Clinic, Seoul, Korea

Correspondence: Sung Bin Cho, Yonsei Seran Dermatology and Laser Clinic, Geumcheon REMAIN CITY 6F, 224 Siheung-daero, Geumcheon-gu, Seoul, 08628, Korea, Tel +82.2-2135-1375, Fax +82.70-8250-1375, Email drscho@gmail.com

Background: Radiofrequency (RF) oscillations generate thermal tissue reactions, the patterns of which vary depending on the mode and efficiency of energy delivery. The aim of our study was to analyze patterns of RF-induced thermal tissue reactions according to the modes of RF delivery, including continuous and gated modes, using an alternating current, invasive bipolar RF device.

Methods: RF energies at frequencies of 1 and 2 MHz were delivered at respective experimental settings into ex vivo bovine liver tissue at a 0.5-mm microneedle penetration depth. The tissue samples were then evaluated thermometrically. A histologic study was performed to evaluate RF-induced thermal tissue reactions at a 3.0-mm microneedle penetration depth.

Results: Thermal imaging study revealed homogenous, well-demarcated, square-shaped zones of RF-induced thermal reactivity on the treated area. Multivariate linear regression analysis revealed that higher temperature elevations immediately after RF treatment (ΔT_1) were positively associated with RF frequency, power, conduction time/pulse pack, and off-time between pulse packs and negatively associated with total off time. In the 1-MHz experimental setting, higher ΔT_1 showed a positive association with power, conduction time/pulse pack, and off-time between pulse packs and a negative association with the number of pulse packs. In the 2-MHz setting, however, higher ΔT_1 was positively associated with only total treatment time.

Conclusion: Thermometric effects during bipolar and gated RF treatments are significantly associated with the frequency, power, and pulse widths and cycles of pulse packs.

Keywords: radiofrequency, bipolar, alternating current, gated pulse, tissue reaction, bovine liver

Introduction

Radiofrequency (RF) oscillations can be delivered to targeted tissues via a continuous or gated mode to generate thermal reactions, the patterns of which depend on the treatment settings and present from the subcellular to the tissue levels.¹⁻⁴ RF delivered at low-temperature hyperthermic conditions at temperatures of 40–45°C induces tissue reactions with reversible cell damage.¹ At temperatures over 60°C, coagulative necrosis occurs with irreversible cytotoxic damage.¹ Therein, the area of coagulative necrosis in the target tissue would theoretically increase over the duration of the RF conduction time. However, when peri-electrode tissue is dehydrated at temperatures around 100°C, further electrical conduction is limited by exponential increases in the impedance of the desiccated tissues.^{1,5} Therefore, many efforts have been made to avoid desiccative tissue reactions and to efficiently deliver RF energy for a proper conduction time.⁵⁻⁷ In doing so, thermal tissue reactions can be produced more uniformly to promote neocollagenesis and collagen remodeling.⁵⁻⁷

Non-invasive bipolar RF devices, which have been clinically used for skin rejuvenation, heat target tissue to achieve therapeutic temperatures in the range of 41–43°C that result in increases in dermal collagen fibers and collagen bundle densities without generating coagulative necrosis.^{6,7} Meanwhile, invasive bipolar RF devices, which deliver RF energy through multiple penetrating electrodes, generate two distinctive zones of RF-induced tissue reaction within the

arrangement of microneedles: 1) zones of coagulative necrosis around the individual tips of invasive microneedles with irreversible cytotoxic damage and 2) zones of non-coagulative subcellular or tissue thermal reactions among the invasive microneedles with reversible cell damage.^{8,9} As such, the clinical efficacy and safety of RF-assisted skin rejuvenation vary depending on the efficiency of energy delivery and the patterns of RF-induced thermal tissue reactions.

In the present study, we comparatively quantified the effects of tissue heating during RF treatments in various experimental settings using an alternating current, invasive bipolar RF device, which has been used for skin rejuvenation and tightening. To do so, we analyzed patterns of RF-induced thermal tissue reactions based on the modes of RF delivery, including continuous and gated modes. RF energies at frequencies of 1 MHz and 2 MHz were delivered at respective experimental settings into ex vivo bovine liver tissue at a 0.5-mm penetration depth for insulated microneedles, and temperature changes elicited in the tissue were thermometrically evaluated. With gated RF delivery, each off-time between pulse packs was regulated to a 20% and 50% conduction time for each pulse pack. RF-induced thermogenic patterns were then evaluated by statistically analyzing thermometric data according to set experimental conditions, particularly pulse widths and cycles. Additionally, a histologic study was performed to evaluate RF-induced thermal tissue reactions at an insulated microneedle penetration depth of 3.0 mm.

Methods

Delivery of Bipolar RF via Insulated Microneedle Electrodes

A bipolar 1- and 2-MHz RF device equipped with insulated microneedle electrodes (VIRTUE RF™; Shenb Co., Ltd., Seoul, Korea) was utilized to evaluate RF tissue reactions on ex vivo bovine liver tissue. When using this device, the treatment parameters, including the RF frequency, penetration depth of microneedles, number of pulse packs, pulse widths of gated on-time and off-time, and level of power, were controlled to fit the study purpose. The device utilizes 10 mm × 10 mm disposable tips (Smart RF™ 36 tips; Shenb Co., Ltd.) composed of 36 insulated microneedle electrodes uniformly arranged in a 6 × 6 pattern. The microneedles are constructed of 24 K gold-plated surgical stainless steel and comprise a body diameter of 300 ± 5 μm and a non-insulated pointed microneedle tip length of 300 μm.

Ex vivo Treatment of Bovine Liver Tissue

For the ex vivo experiment, a total of 80 pieces of fresh bovine liver tissue were prepared at a size of 10 cm × 10 cm × 2 cm/each piece. Prior to delivering invasive bipolar microneedle RF energy, the temperature of ex vivo bovine liver tissue was maintained between 34°C and 36°C in a tissue floating bath. Each tissue specimen was divided into four areas for each experimental setting, and each area was spaced at least 5 cm from the others to minimize RF-induced thermal effects on the other treatment areas. Treatment was performed at microneedle penetration depths of 0.5 mm for thermometric evaluation and 3.0 mm for histologic evaluation. The RF power was set to 4 W and 12 W. The other parameters are summarized in Table 1. All experiments were performed in triplet on different days.

Table 1 Experimental Parameters for 1- and 2-MHz Invasive Bipolar Radiofrequency (RF) Treatment on ex vivo Bovine Liver Tissue

Number of pulse packs	Conduction time/ pulse pack*	Off-time between pulse packs*	Total conduction time*	Total off time*	Total treatment time*
I	100	0	100	0	100
	200	0	200	0	200
	300	0	300	0	300
	400	0	400	0	400
	600	0	600	0	600
	800	0	800	0	800

(Continued)

Table I (Continued).

Number of pulse packs	Conduction time/ pulse pack*	Off-time between pulse packs*	Total conduction time*	Total off time*	Total treatment time*
2	100	50	200	50	250
	200	100	400	100	500
	300	150	600	150	750
	400	200	800	200	1000
	100	20	200	20	220
	200	40	400	40	440
	300	60	600	60	660
	400	80	800	80	880
3	100	20	300	40	340
	200	40	600	80	680
	100	50	300	100	400
	200	100	600	200	800
4	100	50	400	150	550
	200	100	800	300	1100
	100	20	400	60	460
	200	40	800	120	920
6	100	20	600	100	700
	100	50	600	250	850
	200	40	1200	200	1400
	200	100	1200	500	1700
8	100	20	800	140	940
	100	50	800	350	1150
	200	40	1600	280	1880
	200	100	1600	700	2300
10	100	20	1000	180	1180
	100	50	1000	450	1450
	200	40	2000	360	2360
	200	100	2000	900	2900

Note: *Conduction time and off time values are presented in msec.

Thermometric and Histologic Evaluation

Noncontact infrared thermometric measurements of RF-treated ex vivo liver tissue were performed using a thermal imaging camera (FLIR E5; FLIR Systems Inc., Wilsonville, OR, USA). This specified camera comprises 10,800 pixels (120 × 90), covers a temperature range of -20°C to 250°C, and has a thermal sensitivity of less than 0.10°C. Thermal measurements were taken with a thermal imaging camera at baseline and immediately, 10 s, 20 s, 30 s, 40 s,

50 s, and 60 s after RF treatment at a distance of 15 cm between the camera and the surface of the bovine liver specimen.

Immediately after RF treatment at each parameter, biopsy specimens of full thickness from the ex vivo bovine liver tissue were obtained for histologic evaluation. Each sample was fixed in 10% buffered formalin and then embedded in paraffin. The bovine liver tissue blocks were cut longitudinally along the insertion axes of the microneedle electrodes. For each treatment setting, 20 to 30 serial liver tissue sections of 5- μ m thickness were prepared and stained with hematoxylin and eosin.

Statistical Analysis

Data are presented as a mean \pm standard deviation (SD), regression coefficient (B) and standard error (SE). A linear mixed model was used to analyze the effects of each treatment parameter on time-dependent thermometric values. Additionally, linear regression analysis was performed to identify factors associated with thermometric values, and the factors with *P* values under 0.1 in univariate analysis were included in multivariate analysis. *P* values <0.05 were considered statistically significant. All statistical tests were performed using SAS version 9.4 (SAS Institute Inc., Cary, NC, USA).

Results

Thermometric Evaluation of Bipolar 1- and 2-MHz RF-Induced Thermal Tissue Reactions

Thermometric images obtained from a thermal imaging camera revealed elevations in tissue temperature along RF-treated areas in all experimental settings. Homogenous, well-demarcated, square-shaped zones of RF-induced thermal tissue reactivity were macroscopically correlated with the contact surface areas of the 10 mm \times 10 mm disposable tips. Macroscopic thermal tissue reactions became remarkably apparent immediately and at 10 s after bipolar RF treatment and gradually disappeared over 40 s or 60 s. When the thermometric values of baseline tissue temperature were adjusted to 36°C, the average surface temperatures of RF-treated ex vivo bovine liver tissue were estimated as follows: 39.9 \pm 2.5°C at immediately, 37.3 \pm 0.8°C at 10 s, 36.8 \pm 0.6°C at 20 s, 36.5 \pm 0.5°C at 30 s, 36.4 \pm 0.5°C at 40 s, 36.3 \pm 0.4°C at 50 s, and 36.3 \pm 0.4°C at 60 s after RF treatments (*P* < 0.0001 , T_{baseline} vs $T_{\text{immediate}}$, $T_{10\text{s}}$, $T_{20\text{s}}$, $T_{30\text{s}}$, $T_{40\text{s}}$, $T_{50\text{s}}$, and $T_{60\text{s}}$, respectively), where *T* is the surface temperature (°C) of ex vivo bovine liver tissue at specific time points. Therein, the degree of thermal tissue reaction and the duration of retaining heat varied depending on the experimental setting.

Linear regression analyses were performed to identify factors associated with $\Delta T_1 = T_{\text{immediate}} - T_{\text{baseline}}$ and $\Delta T_2 = T_{10\text{s}} - T_{\text{baseline}}$. Therein, a univariate linear regression analysis revealed that higher ΔT_1 was significantly associated with a fewer number of pulse packs, higher RF frequency and power, longer conduction time/pulse pack and off-time between pulse packs, and shorter total off-time (Table 2). Additionally, higher ΔT_2 was significantly associated with a fewer number of pulse packs, higher RF frequency and power, and longer conduction time/pulse pack and off-time between pulse packs. In multivariate linear regression analysis, higher ΔT_1 exhibited a positive association with RF frequency, power, conduction time/pulse pack, and off-time between pulse packs and a negative association with total off-time. Additionally, higher ΔT_2 showed a positive association with RF frequency, power, conduction time/pulse pack, and off-time between pulse packs.

Thermometric Evaluation of Bipolar 1-MHz RF-Induced Thermal Tissue Reactions

When the thermometric values of baseline tissue temperature were adjusted to 36°C, the average surface temperatures of 1-MHz RF-treated ex vivo bovine liver tissue were estimated as follows: 38.8 \pm 2.1°C at immediately, 37.0 \pm 0.8°C at 10 s, 36.6 \pm 0.6°C at 20 s, 36.4 \pm 0.5°C at 30 s, 36.4 \pm 0.5°C at 40 s, 36.3 \pm 0.5°C at 50 s, and 36.2 \pm 0.5°C at 60 s after RF treatments (*P* < 0.0001 , T_{baseline} vs $T_{\text{immediate}}$, $T_{10\text{s}}$, $T_{20\text{s}}$, $T_{30\text{s}}$, $T_{40\text{s}}$, and $T_{50\text{s}}$, respectively; *P* = 0.0003, T_{baseline} vs $T_{60\text{s}}$). Therein, the degree of thermal tissue reaction and the duration of retaining heat varied depending on the experimental setting (Figure 1).

Univariate linear regression analysis revealed that higher ΔT_1 was significantly associated with a fewer number of pulse packs, higher power, and longer conduction time/pulse pack and off-time between pulse packs (Table 3). Additionally, higher ΔT_2 was significantly associated with higher power and longer conduction time/pulse pack and off-

Table 2 Factors Associated with Thermometric Values After 1- and 2-MHz Invasive Bipolar RF Treatments on ex vivo Bovine Liver Tissue in Univariate and Multivariate Linear Regression Analysis

	$\Delta T_1^* = T_{\text{immediate}} - T_{\text{baseline}}$				$\Delta T_2^* = T_{10s} - T_{\text{baseline}}$			
	Univariate		Multivariate		Univariate		Multivariate	
	B (SE)	P value	B (SE)	P value	B (SE)	P value	B (SE)	P value
Frequency	2.819 (0.394)	< 0.0001	2.274 (0.307)	< 0.0001	0.885 (0.142)	< 0.0001	0.804 (0.115)	< 0.0001
Power	0.124 (0.054)	0.0238	0.105 (0.034)	0.0023	0.045 (0.019)	0.0167	0.040 (0.013)	0.0034
Number of pulse packs	-0.426 (0.078)	< 0.0001			-0.084 (0.029)	0.0052		
Conduction time/pulse pack**	0.692 (0.127)	< 0.0001	0.550 (0.090)	< 0.0001	0.201 (0.046)	< 0.0001	0.174 (0.034)	< 0.0001
Off-time between pulse packs**	1.610 (0.462)	0.0007	2.133 (0.341)	< 0.0001	0.628 (0.157)	0.0001	0.634 (0.116)	< 0.0001
Total conduction time**	-0.066 (0.055)	0.2372			0.007 (0.019)	0.7041		
Total off time**	-0.317 (0.131)	0.0174	-0.297 (0.100)	0.0038	-0.026 (0.046)	0.5806		
Total treatment time**	-0.066 (0.041)	0.1098			0.002 (0.014)	0.9114		

Note: *Where T is the surface temperature ($^{\circ}\text{C}$) of ex vivo bovine liver tissue at specific time points, **per 100 msec.

Abbreviations: B, regression coefficient; SE, standard error.

time between pulse packs. In multivariate linear regression analysis, higher ΔT_1 exhibited a positive association with power, conduction time/pulse pack, and off-time between pulse packs and a negative association with the number of pulse packs. Additionally, higher ΔT_2 showed a positive association with power, conduction time/pulse pack, and off-time between pulse packs.

Thermometric Evaluation of Bipolar 2-MHz RF-Induced Thermal Tissue Reactions

When the thermometric values of baseline tissue temperature were adjusted to 36°C , the average surface temperatures of 2-MHz RF-treated ex vivo bovine liver tissue were estimated as follows: $41.6 \pm 1.9^{\circ}\text{C}$ at immediately, $37.8 \pm 0.7^{\circ}\text{C}$ at 10 s, $37.1 \pm 0.4^{\circ}\text{C}$ at 20 s, $36.7 \pm 0.3^{\circ}\text{C}$ at 30 s, $36.5 \pm 0.3^{\circ}\text{C}$ at 40 s, $36.3 \pm 0.3^{\circ}\text{C}$ at 50 s, and $36.3 \pm 0.3^{\circ}\text{C}$ at 60 s after RF treatments ($P < 0.0001$, T_{baseline} vs $T_{\text{immediate}}$, T_{10s} , T_{20s} , T_{30s} , T_{40s} , T_{50s} , and T_{60s} , respectively). Therein, the degree of thermal tissue reaction and the duration of retaining heat varied depending on the experimental setting (Figure 2).

The univariate linear regression analysis revealed that higher ΔT_1 was significantly associated with a greater number of pulse packs and longer conduction time/pulse pack, off-time between pulse packs, total conduction time, total off time, and total treatment time (Table 4). Additionally, higher ΔT_2 was significantly associated with a greater number of pulse packs, longer conduction time/pulse pack, off-time between pulse packs, total conduction time, total off time, and total treatment time. In multivariate analysis, higher ΔT_1 and ΔT_2 were shown to be positively associated with total treatment time, respectively.

Histologic Evaluation of Bipolar RF-Induced Thermal Tissue Reactions

Histologic study to evaluate immediate tissue reactions after RF treatment at a frequency of 1 MHz revealed that RF-induced thermal reactions ranged from mild to marked eosinophilic microscopic changes in the hepatocytes and vasculatures with varying degrees of tissue coagulation within the entire treatment area (Figure 3). The histologic reactions became more apparent with increasing total conduction time and conduction time/pulse pack. Moreover, the histologic reactions were increasingly more apparent along the penetrating vessels and interlobular septum between the area of microneedle electrodes. Experiments with a greater number of pulse packs seemed to generate wider areas of microscopic thermal tissue reactions. Comparing off-time between pulse packs, we noted that a longer off time more frequently elicited a higher degree of RF-induced thermal tissue reactivity than a shorter off time.

Meanwhile, the histologic features of 2-MHz RF-treated tissue specimens included smaller, less clearly demarcated zones of coagulation necrosis around the microneedle tips and more remarkable RF-induced thermal tissue reactions in

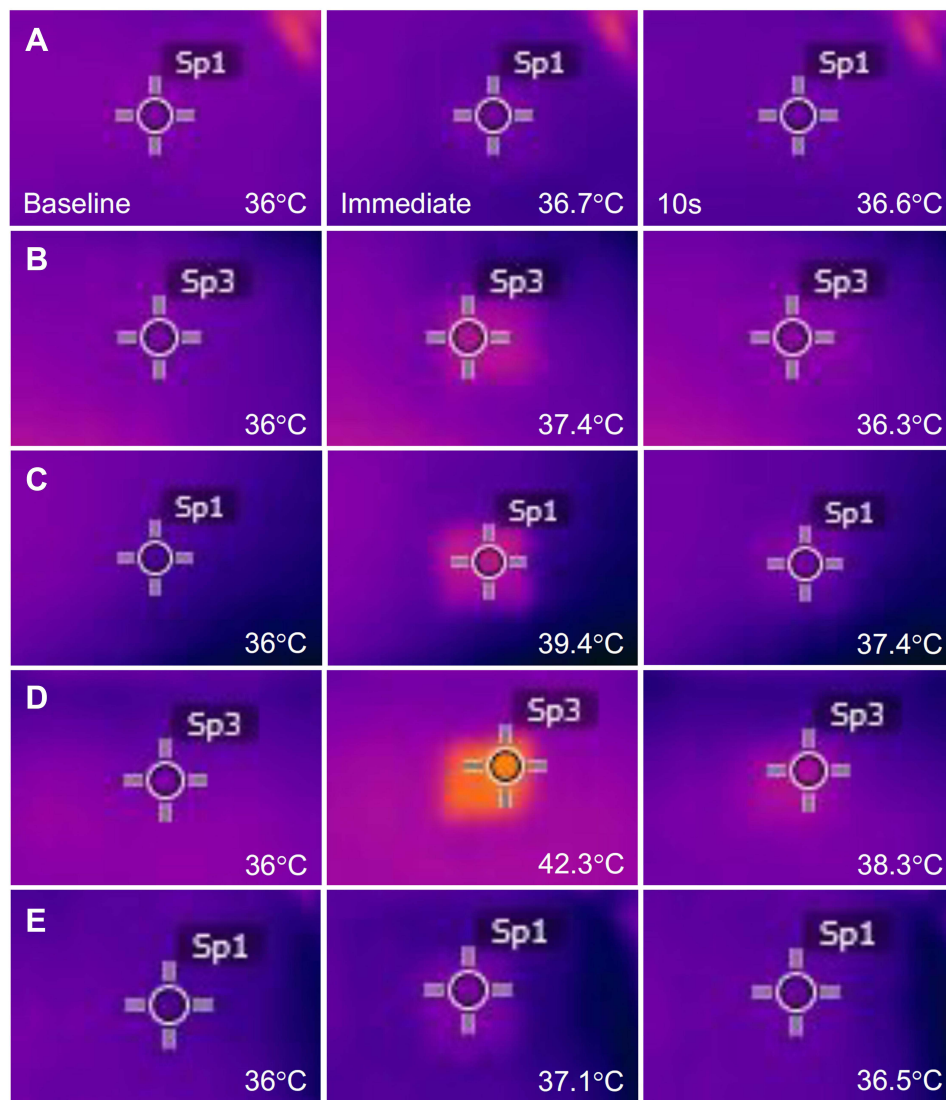


Figure 1 Thermal imaging camera study. Images were captured at baseline, immediately, and 10s after bipolar radiofrequency (RF) treatment at a frequency of 1 MHz. The experimental settings were (A) a power of 4W, a conduction time/pulse pack of 200 msec, and a single pulse pack; (B) 12W, a conduction time/pulse pack of 200 msec, and a single pulse pack; (C) 12W, a conduction time/pulse pack of 600 msec, and a single pulse pack; (D) 12W, a conduction time/pulse pack of 100 msec, 2 pulse packs, an off-time between pulse packs of 50 msec, and a total conduction time of 200 msec; and (E) 12W, a conduction time/pulse pack of 100 msec, two pulse packs, an off-time between pulse packs of 20 msec, and a total conduction time of 200 msec. The thermometric values of baseline tissue were adjusted to 36°C.

the inter-electrode areas, compared with those of 1-MHz RF-treated tissue specimens (Figure 4). The thermal tissue reactions in the areas between microneedle electrodes seemed to become more apparent upon increasing the total conduction time or total treatment time rather than by increasing the conduction time/pulse pack or off-time between pulse packs. Histologic differences in the area and degree of peri-electrode coagulation necrosis among experimental settings were not remarkable, however.

Discussion

In this study, we evaluated patterns of RF-induced thermal tissue reactions based on the modes of RF delivery using an alternating current, invasive bipolar RF device. Herein, a thermal imaging camera study revealed that all experimental settings generated homogeneous, well-demarcated, hyperthermic zones on the surface of ex vivo bovine liver tissue. Histologic studies additionally exhibited remarkable thermal tissue reactions around and between invasive, insulated microneedle electrodes without generating extensive desiccative thermal tissue injury in all experimental settings.

Table 3 Factors Associated with Thermometric Values After 1-MHz Invasive Bipolar RF Treatment on ex vivo Bovine Liver Tissue in Univariate and Multivariate Linear Regression Analysis

	$\Delta T_1^* = T_{\text{immediate}} - T_{\text{baseline}}$				$\Delta T_2^* = T_{10s} - T_{\text{baseline}}$			
	Univariate		Multivariate		Univariate		Multivariate	
	B (SE)	P value	B (SE)	P value	B (SE)	P value	B (SE)	P value
Power	0.155 (0.062)	0.0147	0.155 (0.046)	0.0012	0.056 (0.022)	0.0131	0.056 (0.019)	0.005
Number of pulse packs	-0.337 (0.075)	< 0.0001	-0.249 (0.068)	0.0005	-0.047 (0.030)	0.125		
Conduction time/pulse pack**	0.707 (0.146)	< 0.0001	0.486 (0.134)	0.0006	0.186 (0.056)	0.0015	0.183 (0.051)	0.0006
Off-time between pulse packs**	1.280 (0.551)	0.0234	1.393 (0.408)	0.0011	0.506 (0.194)	0.0114	0.495 (0.171)	0.0051
Total conduction time**	-0.065 (0.053)	0.2273			0.010 (0.019)	0.6083		
Total off time**	-0.244 (0.124)	0.0527			0.002 (0.045)	0.9709		
Total treatment time**	-0.058 (0.039)	0.1376			0.005 (0.014)	0.6992		

Note: *Where T is the surface temperature ($^{\circ}\text{C}$) of ex vivo bovine liver tissue at specific time points, **Per 100 msec.

Accordingly, we were able to perform a thermometric analysis study under the supposition that RF energy at each experimental setting was properly conducted into the ex vivo tissue specimens.

A previous in vivo porcine skin model study compared the patterns of electrocoagulation at frequencies of 1 MHz and 2 MHz using an invasive, alternative current, bipolar microneedle radiofrequency device.¹⁰ Therein, histology data revealed that 2-MHz RF treatments using insulated microneedles resulted in narrower and more concentrated zones of tissue coagulation, compared to 1-MHz treatments.¹⁰ These electrically coagulated areas were positively associated with the level of RF power.¹⁰ Moreover, 1-MHz RF treatments using non-insulated microneedles resulted in patterns of tissue coagulation similar to those achieved with 2-MHz RF treatments using insulated microneedles.¹⁰ The authors suggested that the greater wave period allowed for RF to radiate longer distances and generate tissue electrocoagulation.¹⁰

In our study, univariate and multivariate linear regression analyses revealed that higher RF frequency generated significantly greater ΔT_1 (B[SE] = 2.274 [0.307], $P < 0.0001$) and ΔT_2 (B[SE] = 0.804 [0.115], $P < 0.0001$). Our thermometric data suggest that more RF-induced frictional heat is generated at higher frequencies. However, the variation in electrode impedance with frequency, which affects the deposited power in the tissue at different frequencies, was not controlled in our study. Nonetheless, our histology study revealed that 2-MHz RF treatment generated less coagulation necrosis around the microneedle tips and more remarkable thermal tissue reactions between microneedle electrodes, compared to 1 MHz. Moreover, 2-MHz RF-induced thermal tissue reactions seemed to last longer than those induced by 1-MHz RF. We also suggest that RF treatment at higher frequencies more effectively increases tissue temperature, decreases bioimpedance, and enhances further electrical conduction without generating irreversible coagulative tissue injury.^{1,5} However, the precise association between zones of electrical coagulation and thermometric values remains to be further evaluated.

Our multivariate linear regression analyses revealed that higher power generated significantly greater ΔT_1 (B[SE] = 0.105 [0.034], $P = 0.0023$) and ΔT_2 (B[SE] = 0.040 [0.013], $P = 0.0034$). Interestingly, only 1-MHz RF treatments showed significant associations between power and ΔT_1 (B[SE] = 0.155 [0.046], $P = 0.0012$) and ΔT_2 (B[SE] = 0.056 [0.019], $P = 0.005$) in additional multivariate linear regression analysis. Our findings on power-dependent temperature changes in 1-MHz RF treatment, but not 2-MHz, seemed to be correlated with histology findings of power-dependent size changes in coagulative necrosis zones noted in a previous in vivo porcine skin study.¹⁰

Alternating current, bipolar, and pulsed-type RF treatments have been used to treat senescent fibroblasts, which are associated with various pigmentary disorders.^{11,12} An in vivo hairless mouse study analyzed 2-MHz RF-induced tissue reactions in two different treatment settings: three pulse cycles at a conduction time/pulse pack of 40 msec and five pulse cycles at a conduction time/pulse of 30 msec using invasive non-insulated microneedles.¹³ Therein, a few small zones of coagulative necrosis were found only with a longer conduction time/pulse pack. Nonetheless, RF treatments in both

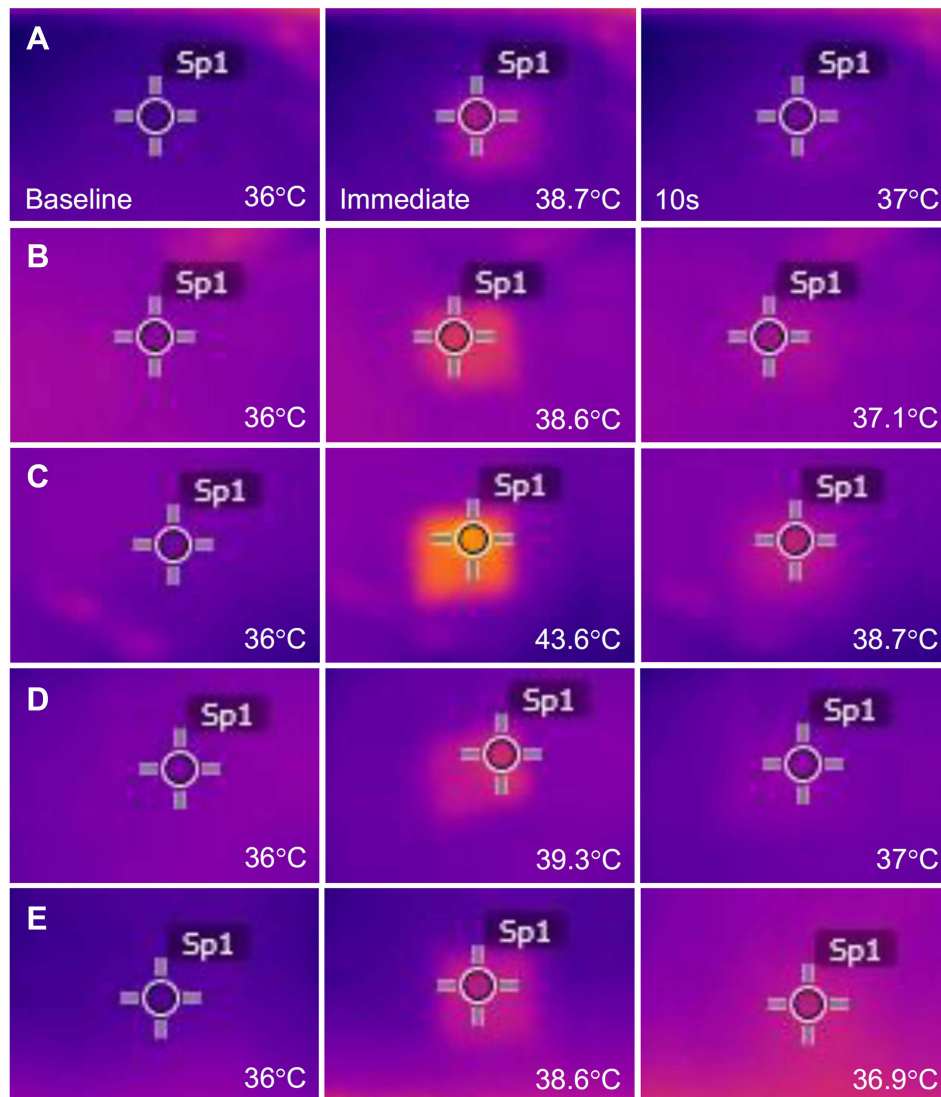


Figure 2 Thermal imaging camera study. Images were captured at baseline, immediately, and 10s after bipolar RF treatment at a frequency of 2 MHz. The experimental settings were (A) a power of 4W, a conduction time/pulse pack of 200 msec, and a single pulse pack; (B) 12W, a conduction time/pulse pack of 200 msec, and a single pulse pack; (C) 12W, a conduction time/pulse pack of 600 msec, and a single pulse pack; (D) 12W, a conduction time/pulse pack of 100 msec, two pulse packs, an off-time between pulse packs of 50 msec, and a total conduction time of 200 msec; and (E) 12W, a conduction time/pulse pack of 100 msec, two pulse packs, an off-time between pulse packs of 20 msec, and a total conduction time of 200 msec. The thermometric values of baseline tissue were adjusted to 36°C.

settings resulted in remarkable changes in the collagen fibers and vascular components in the dermis, notably thickening of the basement membrane.¹³ Accordingly, the efficacy of pulsed-type RF treatment may be insignificantly correlated with zones of RF-induced coagulative necrosis.

In our study, to evaluate the thermometric effects of pulse widths and cycles during pulsed-type RF treatments, we used a longer conduction time/pulse pack, compared to a previous report.¹³ Our multivariate linear regression analysis of 1-MHz RF treatment settings revealed that a higher ΔT_1 holds positive associations with conduction time/pulse pack/100 msec ($B[SE] = 0.486 [0.134]$, $P = 0.0006$) and off-time between pulse packs/100 msec ($B[SE] = 1.393 [0.408]$, $P = 0.0011$) and a negative association with number of pulse packs ($B[SE] = -0.249 [0.068]$, $P = 0.0005$). Additionally, higher ΔT_2 showed positive associations with conduction time/pulse pack/100 msec ($B[SE] = 0.183 [0.051]$, $P = 0.0006$) and off-time between pulse packs/100 msec ($B[SE] = 0.495 [0.171]$, $P = 0.0051$). Meanwhile, a multivariate linear regression analysis of 2-MHz RF treatment settings revealed that a higher ΔT_1 held

Table 4 Factors Associated with Thermometric Values After 2-MHz Invasive Bipolar RF Treatment on ex vivo Bovine Liver Tissue in Univariate and Multivariate Linear Regression Analysis

	$\Delta T_1^* = T_{\text{immediate}} - T_{\text{baseline}}$				$\Delta T_2^* = T_{10s} - T_{\text{baseline}}$			
	Univariate		Multivariate		Univariate		Multivariate	
	B (SE)	P value	B (SE)	P value	B (SE)	P value	B (SE)	P value
Power	0.044 (0.064)	0.4913			0.019 (0.024)	0.4168		
Number of pulse packs	0.604 (0.259)	0.0247			0.230 (0.095)	0.0199		
Conduction time/pulse pack**	0.487 (0.147)	0.0019			0.160 (0.056)	0.0063		
Off-time between pulse packs**	2.034 (0.463)	< 0.0001			0.782 (0.167)	< 0.0001		
Total conduction time**	0.751 (0.059)	< 0.0001			0.269 (0.024)	< 0.0001		
Total off time**	1.425 (0.295)	< 0.0001			0.546 (0.106)	< 0.0001		
Total treatment time**	0.618 (0.047)	< 0.0001	0.618 (0.047)	< 0.0001	0.224 (0.018)	< 0.0001	0.224 (0.018)	< 0.0001

Note: *Where T is the surface temperature ($^{\circ}\text{C}$) of ex vivo bovine liver tissue at specific time points, **per 100 msec.

a positive association with only total treatment time/100 msec ($B[\text{SE}] = 0.618 [0.047]$, $P < 0.0001$) and that a higher ΔT_2 had a positive association with only total treatment time/100 msec ($B[\text{SE}] = 0.224 [0.018]$, $P < 0.0001$).

The histologic study in our report demonstrated different patterns of thermal tissue reactions according to RF frequencies, total conduction time, total treatment time, conduction time/pulse pack, and off-time between pulse packs. However, different tissues have different RF-induced thermal reactions by various experimental factors, including the amount of

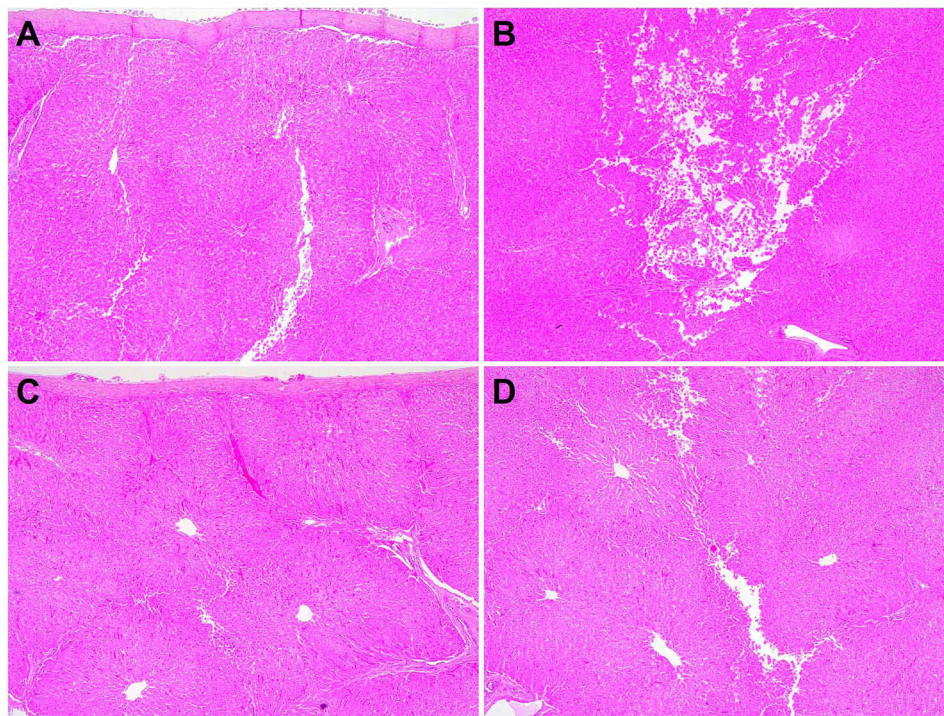


Figure 3 Tissue reactions after 1-MHz bipolar RF treatment on ex vivo bovine liver tissue. The ex vivo bovine liver tissue was treated at experimental settings of (A and B) 12W, a conduction time/pulse pack of 100 msec, three pulse packs, an off-time between pulse packs of 50 msec, and a total conduction time of 300 msec and (C and D) 12W, a conduction time/pulse pack of 100 msec, three pulse packs, an off-time between pulse packs of 20 msec, and a total conduction time of 300 msec. The superficial (A and C) and deeper (B and D) parts of liver tissue specimens exhibit RF-induced tissue reactions at the proximal and distal parts of invasive microneedles, respectively. Hematoxylin & eosin stain. Original magnification x40.

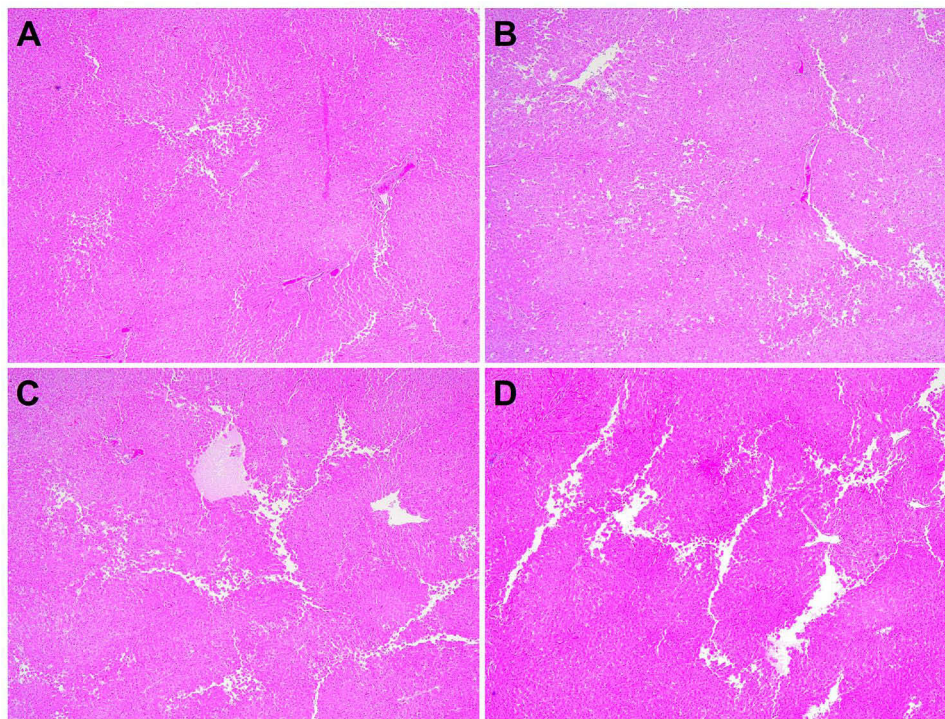


Figure 4 Tissue reactions after 2-MHz bipolar RF treatment on ex vivo bovine liver tissue. The ex vivo bovine liver tissue was treated at experimental settings of (A) 12W, a conduction time/pulse pack of 300 msec, and a single pulse pack; (B) 12W, a conduction time/pulse pack of 400 msec, and a single pulse pack; (C) 12W, a conduction time/pulse pack of 100 msec, three pulse packs, an off-time between pulse packs of 50 msec, and a total conduction time of 300 msec; and (D) 12W, a conduction time/pulse pack of 100 msec, three pulse packs, an off-time between pulse packs of 20 msec, and a total conduction time of 300 msec. Hematoxylin & eosin stain. Original magnification x40.

water in the tissue. Although experiments using ex vivo bovine liver tissue have several limitations in reflecting RF-induced tissue reactions in humans, the more even impedance and permittivity of the liver tissue with hepatocytes and vascular structures during RF delivery, compared with skin with layers and appendage structures, seem to facilitate comparisons of more reproducible RF-induced tissue reactions at various experimental settings.⁹ Nonetheless, because RF treatment at a shorter conduction time/pulse pack than 100 msec generates minimal changes in tissue specimens, in vivo experiments for microscopic, electron microscopic, and molecular biological studies are required to evaluate RF-induced tissue reactions.¹³

In this study, we thermometrically and histologically analyzed the effects of various frequencies, power, number of pulse packs, conduction time/pulse pack, off-time between pulse packs, total treatment time, total conduction time, and total off time during bipolar RF treatment on thermal tissue reactions. Our data revealed that the thermometric effects during bipolar-gated RF treatments are significantly associated with RF power and the pulse widths and cycles of pulse packs. Linear regression analysis revealed that factors correlated with thermometric data differed between RF frequencies. Moreover, RF-induced histologic changes in ex vivo bovine liver tissue were also found to vary depending on the experimental settings. Nonetheless, further controlled, in vivo experimental and clinical studies are necessary to confirm our findings and develop optimized treatment parameters according to medical purposes.

Statement of Ethics

This article does not contain any studies with human participants or animals performed by any of the authors.

Acknowledgments

We thank Anthony Thomas Milliken, ELS at Editing Synthese (<https://editingsynthese.com>) for his assistance with the editing of this manuscript.

Author Contributions

All authors made a significant contribution to the work reported, whether that is in the conception, study design, execution, acquisition of data, analysis and interpretation, or in all these areas; took part in drafting, revising, or critically reviewing the article; gave final approval of the version to be published; have agreed on the journal to which the article has been submitted; and agree to be accountable for all aspects of the work.

Disclosure

The authors declare no conflicts of interest.

References

1. Chu KF, Dupuy DE. Thermal ablation of tumours: biological mechanisms and advances in therapy. *Nat Rev Cancer*. 2014;14:199-208. doi:10.1038/nrc3672
2. Golberg A, Bruinsma BG, Uygun BE, Yarmush ML. Tissue heterogeneity in structure and conductivity contribute to cell survival during irreversible electroporation ablation by “electric field sinks”. *Sci Rep*. 2015;5:8485. doi:10.1038/srep08485
3. Yarmush ML, Golberg A, Serša G, Kotnik T, Miklavčič D. Electroporation-based technologies for medicine: principles, applications, and challenges. *Annu Rev Biomed Eng*. 2014;16:295-320. doi:10.1146/annurev-bioeng-071813-104622
4. Golberg A, Yarmush ML. Nonthermal irreversible electroporation: fundamentals, applications, and challenges. *IEEE Trans Biomed Eng*. 2013;60:707-714. doi:10.1109/TBME.2013.2238672
5. Zhang B, Moser MAJ, Zhang EM, Luo Y, Zhang W. A new approach to feedback control of radiofrequency ablation systems for large coagulation zones. *Int J Hyperthermia*. 2017;33:367-377. doi:10.1080/02656736.2016.1263365
6. Nelson AA, Beynet D, Lask GP. A novel non-invasive radiofrequency dermal heating device for skin tightening of the face and neck. *J Cosmet Laser Ther*. 2015;17:307-312. doi:10.3109/14764172.2015.1039035
7. Boisnic S, Divaris M, Branchet MC, Nelson AA. Split-face histological and biochemical evaluation of tightening efficacy using temperature- and impedance-controlled continuous non-invasive radiofrequency energy. *J Cosmet Laser Ther*. 2017;19:128-132. doi:10.1080/14764172.2016.1262957
8. Zheng Z, Goo B, Kim DY, Kang JS, Cho SB. Histometric analysis of skin-radiofrequency interaction using a fractionated microneedle delivery system. *Dermatol Surg*. 2014;40:134-141. doi:10.1111/dsu.12411
9. Na J, Zheng Z, Dannaker C, Lee SE, Kang JS, Cho SB. Electromagnetic initiation and propagation of bipolar radiofrequency tissue reactions via invasive non-insulated microneedle electrodes. *Sci Rep*. 2015;5:16735. doi:10.1038/srep16735
10. Wooten S, Zawacki ZE, Rheins L, Meschter C, Draelos ZD. An evaluation of electrocoagulation and thermal diffusion following radiofrequency microneedling using an in vivo porcine skin model. *J Cosmet Dermatol*. 2021;20:1133-1139. doi:10.1111/jocd.13690
11. Yoon JE, Kim Y, Kwon S, et al. Senescent fibroblasts drive ageing pigmentation: A potential therapeutic target for senile lentigo. *Theranostics*. 2018;8:4620-4632. doi:10.7150/thno.26975
12. Kim M, Kim SM, Kwon S, Park TJ, Kang HY. Senescent fibroblasts in melasma pathophysiology. *Exp Dermatol*. 2019;28:719-722. doi:10.1111/exd.13814
13. Cho SB, Na J, Zheng Z, et al. In vivo skin reactions from pulsed-type, bipolar, alternating current radiofrequency treatment using invasive noninsulated electrodes. *Skin Res Technol*. 2018;24:318-325. doi:10.1111/srt.12433

Clinical, Cosmetic and Investigational Dermatology

Dovepress

Publish your work in this journal

Clinical, Cosmetic and Investigational Dermatology is an international, peer-reviewed, open access, online journal that focuses on the latest clinical and experimental research in all aspects of skin disease and cosmetic interventions. This journal is indexed on CAS. The manuscript management system is completely online and includes a very quick and fair peer-review system, which is all easy to use. Visit <http://www.dovepress.com/testimonials.php> to read real quotes from published authors.

Submit your manuscript here: <https://www.dovepress.com/clinical-cosmetic-and-investigational-dermatology-journal>